Comparative Study of Linear and Nonlinear Thermal Radiation on Casson Dusty Fluid Flow Over a Convectively Heated Stretching Sheet

Manjula K. M.[1]; Y. Veeranna[2]

[1]Department of Mathematics, Government First Grade College, Channarayapatna-573116, Karnataka, India
[2]Department of Studies and Research in Mathematics, Government Science College (Autonomous), Bengaluru-560 001, Karnataka, India

Publication Date: 2026/09/07

Abstract: The present study investigates the influence of linear and nonlinear thermal radiation on Casson dusty fluid flow over a stretching sheet in the presence of heat generation effects. The flow model incorporates viscous dissipation, convective boundary condition, exponential heat generation, and volumetric heat source effects. The governing partial differential equations describing the fluid and dust phases are transformed into a coupled system of nonlinear ordinary differential equations using suitable similarity transformations. The resulting equations are solved numerically with the aid of the Runge-Kutta-Fehlberg (RKF) method together with the shooting technique. The effects of important physical parameters on the velocity and temperature distributions are examined in detail. The numerical results reveal that increasing the Casson fluid parameter suppresses the velocity profiles while enhancing the thermal field. It is further observed that larger values of the radiation parameter, Biot number, Eckert number, and heat generation parameters significantly increase the temperatures of both fluid and dust phases. Moreover, nonlinear radiation produces a stronger thermal enhancement compared to linear radiation. The present investigation is useful in understanding thermal transport processes in engineering applications involving radiative heat transfer, particulate suspensions, thermal energy systems, electronic cooling, and metallurgical processes.

Keywords: *Casson Fluid; Dusty; Thermal Radiation; Viscous Dissipation; Irregular Heat Source.*

How to Cite: Manjula K. M.; Y. Veeranna (2026) Comparative Study of Linear and Nonlinear Thermal Radiation on Casson Dusty Fluid Flow Over a Convectively Heated Stretching Sheet. *International Journal of Innovative Science and Research Technology*, 11(8), 2979-2987. https://doi.org/10.38124/ijisrt/26aug1557

I. INTRODUCTION

Thermal radiation has become an important area of research due to its crucial role in controlling heat transfer in several engineering and industrial processes. Applications such as nuclear reactors, thermal power systems, solar energy devices, high-temperature manufacturing, electronic cooling, and aerospace engineering frequently involve radiative heat transfer effects. Motivated by these applications, many researchers have examined fluid flow and heat transfer in the presence of thermal radiation under different physical conditions (Makinde [1], Mushtaq et al. [2], Sreedevi et al. [3], Gireesha et al. [4], Sampath Kumar et al. [5], Jyoti et al. [6]). Nevertheless, the majority of these investigations are based on the assumption of linear thermal radiation, which is valid only for flows involving relatively small temperature differences. In practical thermal systems, however, large temperature variations are often encountered, making the linear approximation insufficient for accurate prediction of heat transfer behavior. Consequently, nonlinear thermal radiation has attracted considerable interest in recent years because it provides a more realistic representation of radiative heat transport in high-temperature environments. Pantokratoras et al. [7] investigated Sakiadis flow with nonlinear Rosseland thermal radiation and demonstrated that nonlinear radiation considerably modifies the thermal boundary layer structure compared with the linear radiation case. Cortell [8] later analyzed flow and heat transfer over a stretching sheet considering nonlinear thermal radiation effects. While Hayat et al. [9] explored three-dimensional hydromagnetic viscoelastic fluid flow under nonlinear thermal radiation. Nonlinear convective and radiated flow of tangent hyperbolic liquid due to stretched surface with convective condition numerically investigated by Mahanthesh et al. [10]. Additional contributions and detailed discussions on nonlinear thermal radiation can be found in the works of (Refer [11-14])

The study of non-Newtonian fluid flow has attracted considerable interest due to its important role in many engineering and industrial processes. Unlike Newtonian fluids, non-Newtonian fluids exhibit complex rheological

ISSN No:-2456-2165 https://doi.org/10.38124/ijisrt/26aug1557

characteristics such as variable viscosity, yield stress, and shear-dependent behavior. To describe these complex flow properties, several mathematical models have been proposed in the literature, including the Carreau-Yasuda, Casson, Cross, Maxwell, Powell-Eyring, Prandtl-Eyring, Ellis, Jeffery, and generalized power-law models [15-17]. These models have been widely utilized to analyze fluid transport phenomena under different physical conditions and geometrical configurations. Among the various non-Newtonian fluid models, the Casson fluid model introduced by Casson [18] in 1959 has received significant attention because of its ability to represent the behavior of yield stress fluids. The Casson model is particularly useful in describing the flow of suspensions, emulsions, biological fluids, and blood flow at low shear rates. Due to these characteristics, Casson fluids have numerous applications in biomedical engineering, food processing, cosmetic manufacturing, pharmaceutical industries, and petroleum engineering. Several investigations related to Casson fluid flow have been reported in recent years. Mukhopadhyay et al. [19] analyzed the unsteady two-dimensional flow of Casson fluid over a stretching surface with prescribed thermal conditions. Nandeppanavar et al. [20] examined the steady flow of Casson nanofluid over an exponentially stretching sheet and observed a reduction in fluid velocity with increasing Casson parameter values. Awais et al. [21] studied the effects of heat and mass transfer on MHD Casson fluid flow through a porous medium over a shrinking surface. In addition, numerous studies concerning Casson fluid and Casson nanofluid flow under different physical situations have been presented in Refs. [22-26].

Dusty fluid flow has attracted significant attention because of its important applications in engineering and industrial processes. A dusty fluid consists of a fluid containing suspended solid particles, where the interaction between the fluid and particle phases strongly influences the momentum and heat transfer characteristics. Such flows are encountered in combustion systems, aerosol transport, geothermal engineering, petroleum industries, nuclear reactors, and powder processing technologies. Owing to its practical importance, dusty fluid flow under various physical and thermal conditions has attracted considerable attention from researchers in recent years [27-33].

Although several studies have been reported on Casson fluid flow, dusty fluid flow, and thermal radiation effects, comparatively little attention has been devoted to the combined analysis of Casson dusty fluid flow over a convectively heated stretching sheet in the presence of both linear and nonlinear thermal radiation. Moreover, most of the existing investigations are limited to either single-phase Casson fluids or linear radiation models, while the comparative influence of linear and nonlinear radiation on fluid and dust phase heat transfer characteristics has not been adequately addressed. In practical thermal engineering systems involving particulate suspensions, high-temperature manufacturing processes, thermal energy devices, electronic cooling systems, and metallurgical operations, the interaction between dust particles, magnetic field, and nonlinear radiative heat transfer plays a significant role in controlling the transport phenomena. Motivated by these observations, the present work aims to examine the effects of nonlinear thermal radiation on Casson dusty fluid flow over a convectively heated stretching sheet together with heat generation mechanisms and viscous dissipation. Particular emphasis is given to comparing the thermal behavior under linear and nonlinear radiation conditions in order to provide a better understanding of heat transfer enhancement in dusty fluid transport systems.

➤ *Mathematical Formulation*

Consider a steady, two-dimensional boundary layer flow of an incompressible and electrically conducting Casson fluid containing suspended dust particles over a stretching sheet. A Cartesian coordinate system is selected such that the (x)-axis is taken along the surface of the sheet, while the (y)-axis is normal to it. The sheet is stretched with a linear velocity $(U_w = bx)$, where $(b > 0)$ is the stretching rate parameter. The flow is generated due to the application of two equal and opposite forces along the (x)-direction while keeping the origin fixed, and the flow region is restricted to $(y > 0)$. A convective heating condition is imposed at the sheet surface, where the lower side of the sheet is heated by a hot fluid of constant temperature (T_f), while (T_∞) represents the ambient temperature far away from the surface. In addition, the effects of thermal radiation are taken into account in the energy transport process to analyze the influence of radiative heat transfer on the fluid and dust phase temperatures. The physical configuration of the problem is illustrated in Figure 1.

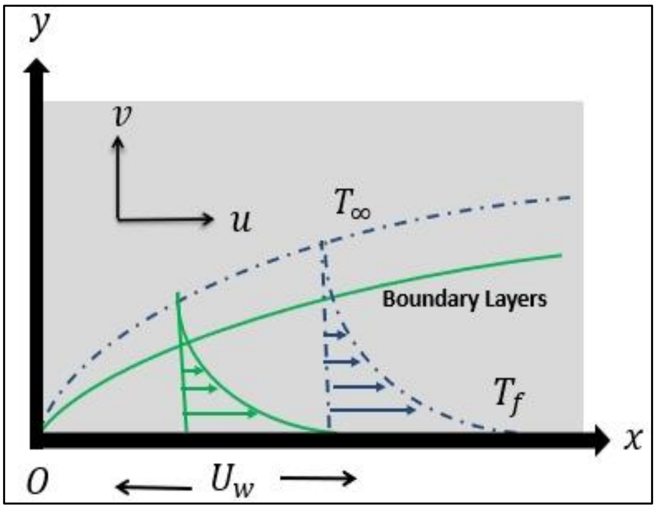

Fig 1 Schematic Diagram of Problem.

The simplified two-dimensional boundary layer equations of continuity, momentum and heat transport for both fluid phase and dust phase with usual notations are;

➤ *Casson Fluid Phase:*

$$\frac{\partial u}{\partial x} + \frac{\partial v}{\partial y} = 0, \tag{1}$$

$$u\frac{\partial u}{\partial x} + v\frac{\partial u}{\partial y} = \nu\left(1 + \frac{1}{\beta}\right)\frac{\partial^2 u}{\partial y^2} + \frac{KN}{\rho}(u_p - u) \tag{2}$$

ISSN No:-2456-2165 https://doi.org/10.38124/ijisrt/26aug1557

$$\rho Cp\left(u\frac{\partial T}{\partial x}+v\frac{\partial T}{\partial y}\right)=k\frac{\partial^2 T}{\partial y^2}+\frac{\rho_p c_m}{\tau_T}(T_p-T)+\mu\left(\frac{\partial u}{\partial y}\right)^2+Q_T(T-T_\infty)$$

$$-\frac{\partial q_r}{\partial y}+Q_E(T_f-T_\infty)\exp\left(-n\sqrt{\frac{b}{\nu}}y\right), \quad (3)$$

➢ *Dust Phase:*

$$\frac{\partial u_p}{\partial x}+\frac{\partial v_p}{\partial y}=0, \quad (4)$$

$$u_p\frac{\partial u_p}{\partial x}+v_p\frac{\partial u_p}{\partial y}=\frac{KN}{\rho_p}(u-u_p), \quad (5)$$

$$\left(u_p\frac{\partial T_p}{\partial x}+v_p\frac{\partial T_p}{\partial y}\right)=\frac{1}{\tau_T}(T-T_p), \quad (6)$$

Where x and y denote the cartesian co-ordinates, (u,v) and (u_p,v_p) are velocity components of fluid and dust phase along x and y directions respectively, β -Casson fluid parameter, ν -kinematic viscosity coefficient, ρ and ρ_p -density of the fluid and dust particle respectively, $K=6\pi\mu r$ -strokes drag coefficient, N-number density of dust particles, μ dynamic viscosity of fluid, r radius of dust particle, k-thermal conductivity of the fluid, T_∞-uniform ambient temperature, T and T_p-temperature of fluid and dust particle, Q_E-exponential heat source, Q_T -heat generation source, q_r -radiative heat flux, k -thermal conductivity of the fluid, B_0-magnetic field, C_p-specific heat capacity at constant pressure, C_m-specific heat of dust particle, τT -relaxation time of the dust particle, σ-electrical conductivity.

The heat flow expression for thermal radiation, as approximated by the Rosseland approximation, is:

$$q_r=-\frac{16\sigma^*}{3k_1}T^3\frac{\partial T}{\partial z}, \quad (7)$$

The symbol σ^* is constant according to the Stefan–Boltzmann whereas the mean absorption coefficient is k_1. Equation (7) in (3) yielded:

$$\rho Cp\left(u\frac{\partial T}{\partial x}+v\frac{\partial T}{\partial y}\right)=k\frac{\partial^2 T}{\partial y^2}+\frac{\rho_p c_m}{\tau_T}(T_p-T)+\mu\left(\frac{\partial u}{\partial y}\right)^2+Q_T(T-T_\infty)$$

$$+\frac{16\sigma^*}{3k_1}\frac{\partial}{\partial y}\left(T^3\frac{\partial T}{\partial z}\right)+Q_E(T_f-T_\infty)\exp\left(-n\sqrt{\frac{b}{\nu}}y\right), \quad (8)$$

The relevant boundary conditions are;

$$u=U_w, v=0, -k\frac{\partial T}{\partial y}=h_f(T-T_f) \text{ at } y=0,$$

$$u\to 0, u_p\to 0, v_p\to v, T\to T_\infty, T_p\to T_\infty \text{ as } y\to\infty \quad (9)$$

Introduce the following similarity transformations:

$$u=bxf'(\xi),\ v=-\sqrt{\nu b}\,f(\xi),\ \xi=\sqrt{\frac{b}{\nu}}y,\ u_p=bxF'(\xi),\ v_p=-\sqrt{\nu b}\,F(\xi),$$

$$T=T_\infty+(T_f-T_\infty)\theta(\xi),\ T_p=T_\infty+(T_f-T_\infty)\theta_p(\xi) \quad (10)$$

Using the transformations, into equations (2), (5), (6) and (7) yeild;

$$\left(1+\frac{1}{\beta}\right)f'''+ff''-f'^2+l\beta_v(F'-f')-Mf'=0 \quad (11)$$

$$F''F-F'^2+\beta_v(f'-F')=0, \quad (12)$$

$$((1+R(1+(\theta_w-1)\theta)^3)\theta')'+Prf\theta'+l\gamma\beta_t Pr(\theta p-\theta)+PrQ_t\theta$$

$$EcPr(f'')^2+PrQ_e\exp(-\xi n)=0, \quad (13)$$

$$\theta_p{}'F-\beta_t(\theta_p-\theta)=0. \quad (14)$$

Reduced boundary conditions are:

$$f(\xi)=0,\ f'(\xi)=1,\ \theta'(\xi)=-Bi(1-\theta) \text{ at } \xi=0,$$

$$F'(\xi)\to 0,\ f'(\xi)\to 0,\ F(\xi)\to f(\xi),\ \theta(\xi)\to 0,\ \theta_p(\xi)\to 0 \text{ as } \xi\to\infty \quad (15)$$

Where β -casson fluid parameter, M-magnetic parameter, l-mass concentration of dust particles, β_v-fluid particle interaction parameter for velocity, Pr- Prandtl number, β_t-fluid particle interaction parameter for temperature, Q_t- thermal dependent heat source parameter, R -nonlinear thermal radiation parameter, θ_w -temperature ratio parameter, Re_x -Reynolds number, Q_e-exponential source dependent heat source, Ec -Eckert number, Bi -Biot number. They are defined as;

$$l=\frac{mN}{\rho}, \beta_v=\frac{1}{b\tau_v}, \tau_v=\frac{m}{K}, Re_x=\frac{U_W^2}{b\nu}, \gamma=\frac{C_m}{C_p}, Re_x=\frac{Uwb^2}{\nu}$$

$$R=\frac{16\,\sigma T_\infty{}^3}{3k_1k},\ \theta_w=\frac{T_f}{T_\infty}, Ec=\frac{U_W^2}{C_p(T_f-T_\infty)}, Bi=\frac{h_f}{k}\sqrt{\nu\backslash b},$$

$$Pr=\frac{\mu C_p}{k}, \beta_t=\frac{1}{b\tau_t}, Q_t=\frac{Q_T}{\rho C_p b}, Q_e=\frac{Q_E}{\rho C_p b}$$

The skin friction coefficient and Nusselt number in non-dimentional form are:

$$\sqrt{Re_x}C_f=\left(1+\frac{1}{\beta}\right)f''(0), \quad (16)$$

$$\frac{Nu}{\sqrt{Re_x}}=-(1+R\theta_w{}^3)\theta'(0), \quad (17)$$

➢ *Numerical Scheme*

The nonlinear coupled ordinary differential equations given in equations (11)-(14), together with the associated boundary conditions (15), are solved numerically by employing the Runge-Kutta-Fehlberg shooting technique. For computational convenience, the governing higher-order equations are transformed into a system of first-order differential equations through the following substitutions:

$$f=y_1, f'=y_2, f''=y_3, F=y_4, F'=y_5, \theta=y_6, \theta'=y_7, \theta_p=y_8$$

ISSN No:-2456-2165 https://doi.org/10.38124/ijisrt/26aug1557

Accordingly, the transformed first-order system becomes:

$$y_1{}' = y_2$$

$$y_2{}' = y_3$$

$$y_3' = \frac{\beta}{1+\beta}\left(y_2^2 - y_1 y_3 - l\beta_v(y_5 - y_2) + My_2\right)$$

$$y_4{}' = y_5$$

$$y_5' = \frac{1}{y_4}\{y_5^2 - \beta_v(y_2 - y_5)\}$$

$$y_6{}' = y_7$$

$$y_7' = -\frac{\{Pry_1y_7 + l\gamma\beta\square Pr(y_8 - y_6) + PrQ\square y_6 + EcPr(y_3)^2 + PrQ_e e^{-(\xi^n)}\}}{\{1 + R(1 + (\theta w - 1)y_6)^3\}}$$

$$y_8{}' = \left(\frac{\beta\square}{y_4}\right)(y_8 - y_6)$$

The corresponding boundary conditions are:

$$y_1(0) = 0, \quad y_2(0) = 1, \quad y_3(0) = s_1$$

$$y_4(0) = s_2, \quad y_5(0) = s_3$$

$$y_6(0) = s_4, \quad y_7(0) = -Bi(1 - y_6(0))$$

$$y_8(0) = s_5$$

Where $(s_1, s_2, s_3, s_4,)$ and (s_5) are the unknown initial guesses evaluated iteratively through the shooting procedure. After transforming the boundary value problem into an equivalent initial value problem, the resulting equations are integrated numerically using the RKF method. The computations are performed with a step size $\Delta\eta = 0.001$ and convergence tolerance 10^{-6}.

II. RESULTS AND DISCUSSION

The effects of the governing physical parameters on the velocity and temperature profiles are illustrated graphically, whereas the variations in the skin-friction coefficient and local Nusselt number are presented through tables. Special attention is given to the influence of the Casson fluid parameter (β), radiation parameter (R), Eckert number (Ec), volumetric heat generation parameter (Q_t), and exponential heat generation parameter (Q_e). Unless otherwise stated, the numerical computations are performed for the fixed parameter values $\beta = 1.5, Bi = 0.5, \beta t = \beta v = 0.8, Ec = 0.9, Qe = Qt = 0.2, R = 0.3, l = 0.6,\ \theta w\, 2$. Furthermore, the effects of selected physical parameters on the skin-friction coefficient and local Nusselt number are summarized in Tables 1 and 2. Figure 2 present the influence of the Casson fluid parameter (β) on the velocity and temperature distributions of both fluid and dust phases. It is observed from the velocity profiles that increasing the Casson parameter reduces the fluid velocity in both phases. Physically, larger values of (β) enhance the yield stress of the Casson fluid, which strengthens the resistance to fluid motion and consequently suppresses the momentum boundary layer development. The effects of the Casson parameter on the temperature distributions for both fluid and dust phases are displayed in figure 3. It is noticed that the temperature profiles increase with increasing values of (β). The enhancement in temperature is attributed to the increase in fluid resistance, which weakens the fluid motion and reduces the rate of heat transport away from the surface. As a result, thermal energy accumulates within the boundary layer region, leading to higher temperatures and thicker thermal boundary layers. Figures 4 and 5 illustrate the influence of the Biot number (Bi) and Eckert number (Ec) on the temperature distributions of both the fluid phase $(\theta(\xi))$ and dust phase $(\theta_p(\xi))$ under linear and nonlinear thermal radiation conditions. It is observed from Figure 4 that increasing values of the Biot number significantly enhance the temperature profiles in both phases. Physically, a larger Biot number corresponds to stronger convective heating at the sheet surface, which supplies more thermal energy to the fluid and consequently thickens the thermal boundary layer. Furthermore, the temperature distributions obtained in the presence of nonlinear radiation are comparatively higher than those corresponding to linear radiation, indicating that nonlinear radiation contributes additional heat energy to the system. Figure 5 depicts the variation of temperature profiles for different values of the Eckert number (Ec). It is clear that the temperatures of both the fluid and dust phases increase with increasing (Ec). This behavior occurs because the Eckert number represents the conversion of kinetic energy into internal energy through viscous dissipation. As viscous dissipation becomes stronger, additional heat is generated within the fluid, leading to an enhancement in the thermal boundary layer thickness. Moreover, nonlinear radiation produces relatively higher temperature distributions compared to linear radiation throughout the flow domain. Overall, the combined influence of convective heating, viscous dissipation, and nonlinear radiation intensifies the thermal field more effectively than the linear radiation case.

Figures 6 and 7 depict the effects of the exponential heat generation parameter (Q_e) and volumetric heat generation parameter (Q_t) on the temperature distributions for both fluid and dust phases. It is observed that the temperature profiles increase substantially with increasing values of (Q_e) and (Q_t). Physically, larger heat generation parameters introduce additional thermal energy into the fluid domain, which increases the internal energy of the system. As a result, the thermal boundary layer becomes thicker and the temperature of both phases rises considerably. Furthermore, the stronger heat generation mechanism weakens the rate of heat dissipation from the surface, leading to an overall enhancement in the thermal field.

Figure 8 demonstrates the influence of the radiation parameter (R) on the temperature distributions of both the fluid phase $(\theta(\xi))$ and dust phase $(\theta_p(\xi))$ under linear and nonlinear radiation conditions. It is observed that the temperature profiles increase significantly with increasing values of the radiation parameter. Physically, larger values of (R) enhance the radiative heat flux within the fluid region, which supplies additional thermal energy to the system and

ISSN No:-2456-2165 https://doi.org/10.38124/ijisrt/26aug1557

consequently raises the temperatures of both phases. As a result, the thermal boundary layer thickness becomes larger for higher radiation levels. Moreover, the effect of nonlinear radiation is found to be more pronounced compared to linear radiation, as the corresponding temperature distributions remain considerably higher throughout the boundary layer region. This indicates that nonlinear thermal radiation contributes more effectively to heat transfer enhancement in the Casson dusty fluid flow system. Tables 1 and 2 present the variations in the skin-friction coefficient and local Nusselt number for different values of the Casson fluid parameter (β), radiation parameter (R), exponential heat generation parameter (Q_e), and volumetric heat generation parameter (Q_t) under both linear and nonlinear radiation conditions. From Table 1, it is observed that increasing values of the Casson parameter reduce the magnitude of the skin-friction coefficient and local Nusselt number for both radiation cases. Physically, larger Casson parameter enhances the yield stress of the fluid, which suppresses the fluid motion and weakens the heat transfer rate. In contrast, increasing the radiation parameter significantly enhances the local Nusselt number, particularly in the nonlinear radiation case, indicating stronger thermal transport due to enhanced radiative heat flux. Table 2 reveals that higher values of the heat generation parameters (Q_e) and (Q_t) decrease the local Nusselt number for both linear and nonlinear radiation conditions, owing to the accumulation of thermal energy within the boundary layer. Moreover, nonlinear radiation consistently produces higher heat transfer rates compared to linear radiation, demonstrating its stronger contribution to the thermal enhancement of the Casson dusty fluid flow system.

Overall, the present investigation reveals that nonlinear radiation produces a stronger enhancement in the thermal field compared to linear radiation, leading to higher temperature distributions and thicker thermal boundary layers in both fluid and dust phases. These findings are significant in several engineering and industrial applications involving high-temperature heat transfer processes, such as thermal energy systems, solar collectors, nuclear reactors, cooling of electronic devices, metallurgical operations, and particulate transport systems where radiative effects and dust particle interactions play an important role.

Table 1 Variations in the Skin Friction Coefficient and Local Nusselt Number for Different Values β and R for Linear and Non-Linear Radiation.

$\boldsymbol{\beta}$	$\boldsymbol{R}$	**Linear Radiation**		**Nonlinear radiation**	
		$\boldsymbol{C_f Re_x^{1/2}}$	$\boldsymbol{Nu_x Re_x^{-1/2}}$	$\boldsymbol{C_f Re_x^{1/2}}$	$\boldsymbol{Nu_x Re_x^{-1/2}}$
0.5		-1.97235	0.209794	-1.97235	0.605493
1.0		-1.60607	0.167219	-1.60607	0.518872
1.5		-1.46524	0.142955	-1.46524	0.471081
	0.3	-1.46524	0.142955	-1.46524	0.471081
	0.6	-1.46524	0.183422	-1.33840	0.850255
	1.0	1.46524	0.236234	-1.33840	1.062603

Table 2 Variations in the Skin Friction Coefficient and Local Nusselt Number for Different Values Q_e and Q_t for Linear and Non-Linear Radiation.

$\boldsymbol{Q_e}$	$\boldsymbol{Q_t}$	**Linear Radiation**		**Nonlinear radiation**	
		$\boldsymbol{C_f Re_x^{1/2}}$	$\boldsymbol{Nu_x Re_x^{-1/2}}$	$\boldsymbol{C_f Re_x^{1/2}}$	$\boldsymbol{Nu_x Re_x^{-1/2}}$
0.1		-1.46524	0.283420	-1.33840	0.798757
0.4		-1.46524	0.142955	-1.46524	0.471081
0.8		-1.46524	0.002490	-1.33840	0.272228
	0.1	1.46524	0.213124	-1.33840	0.644400
	0.4	-1.46524	0.142955	-1.46524	0.471081
	0.8	1.46524	0.042970	-1.33840	0.362114

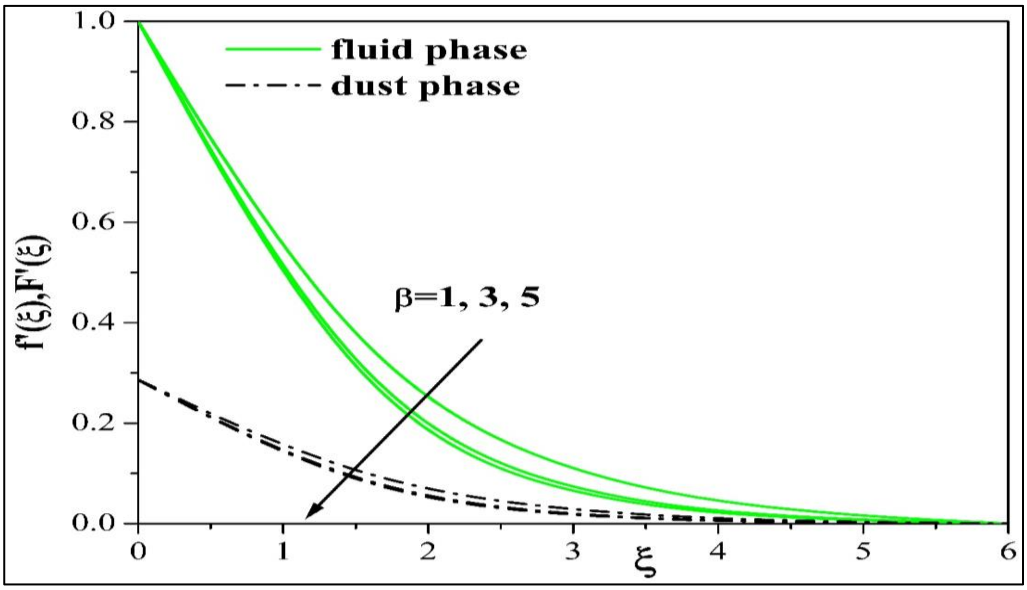

Fig 2 Influence of the Casson Fluid Parameter (β) on the Velocity Distributions of the Fluid Phase $f'(\xi)$ and Dust Phase $F'(\xi)$.

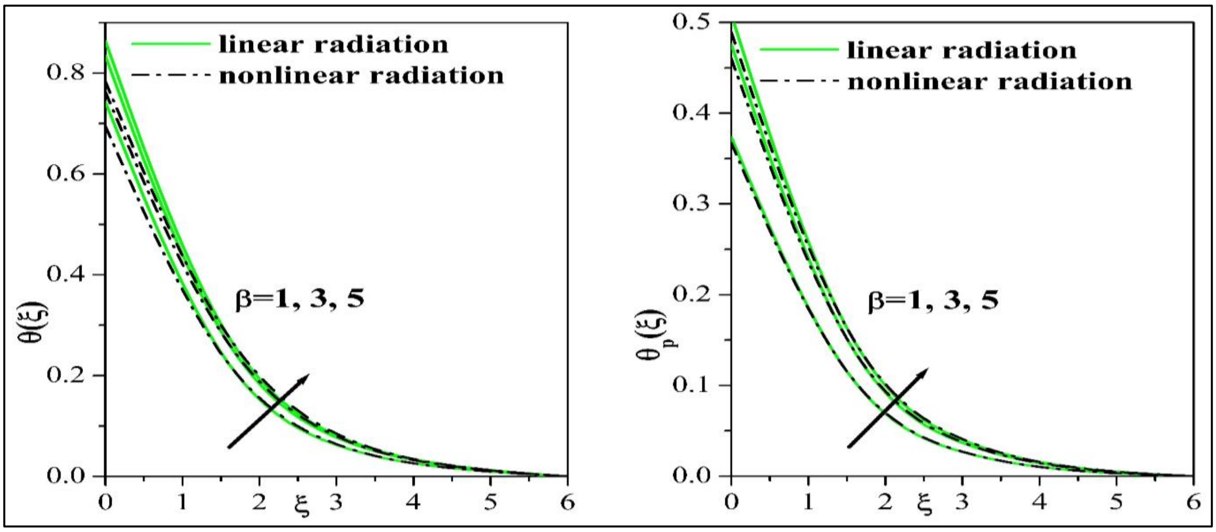

Fig 3 Influence of the Casson Fluid Parameter (β) on the Temperature Distributions of the Fluid Phase $\theta(\xi)$ and Dust Phase $\theta_p(\xi)$.

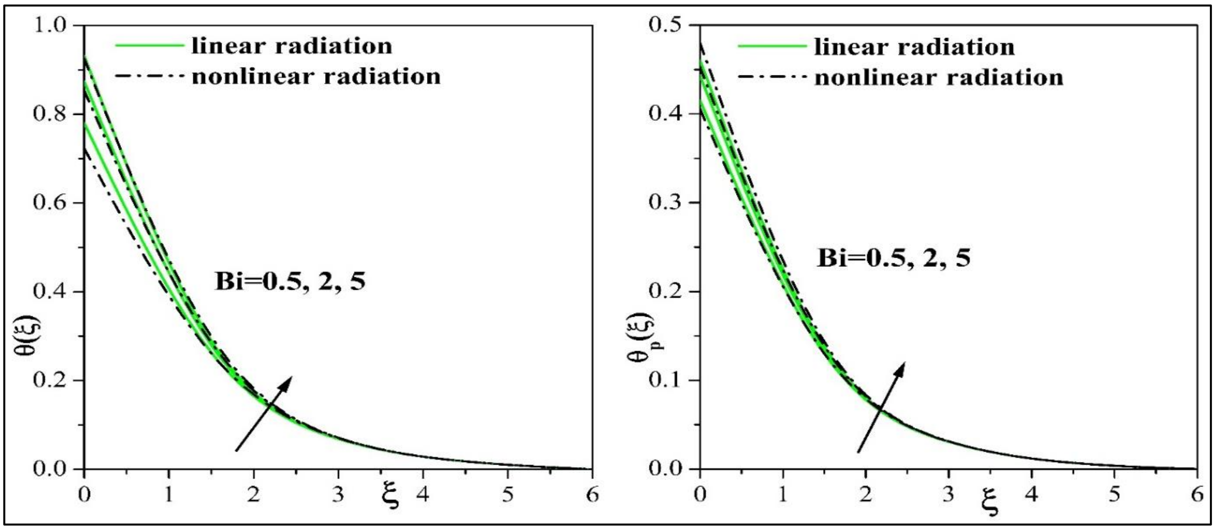

Fig 4 Influence of the Biot Number (Bi) on the Temperature Distributions of the Fluid Phase $\theta(\xi)$ and Dust Phase $\theta_p(\xi)$.

ISSN No:-2456-2165 https://doi.org/10.38124/ijisrt/26aug1557

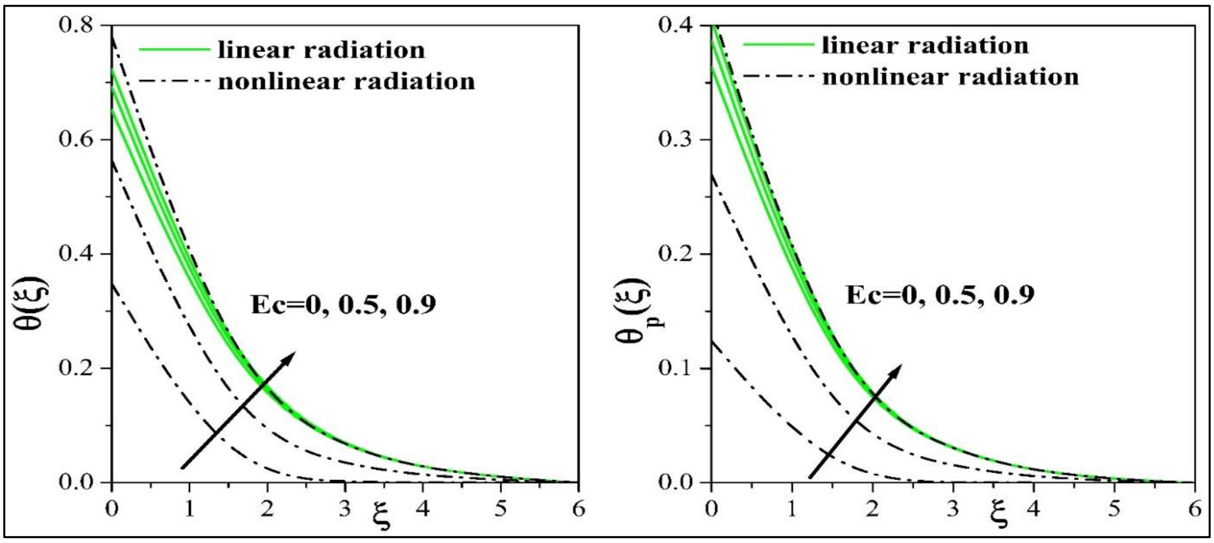

Fig 5 Influence of the (Ec) on the Temperature Distributions of the Fluid Phase $\theta(\xi)$ and Dust Phase $\theta_p(\xi)$.

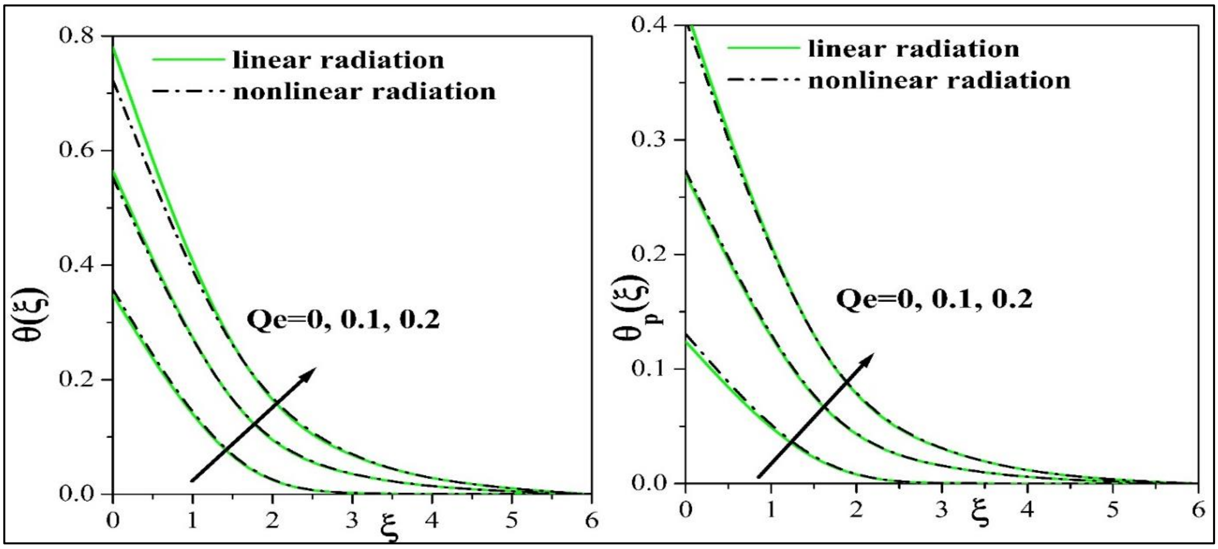

Fig 6 Influence of the Exponential Heat Source (Q_e) on the Temperature Distributions of the Fluid Phase $\theta(\xi)$ and Dust Phase $\theta_p(\xi)$.

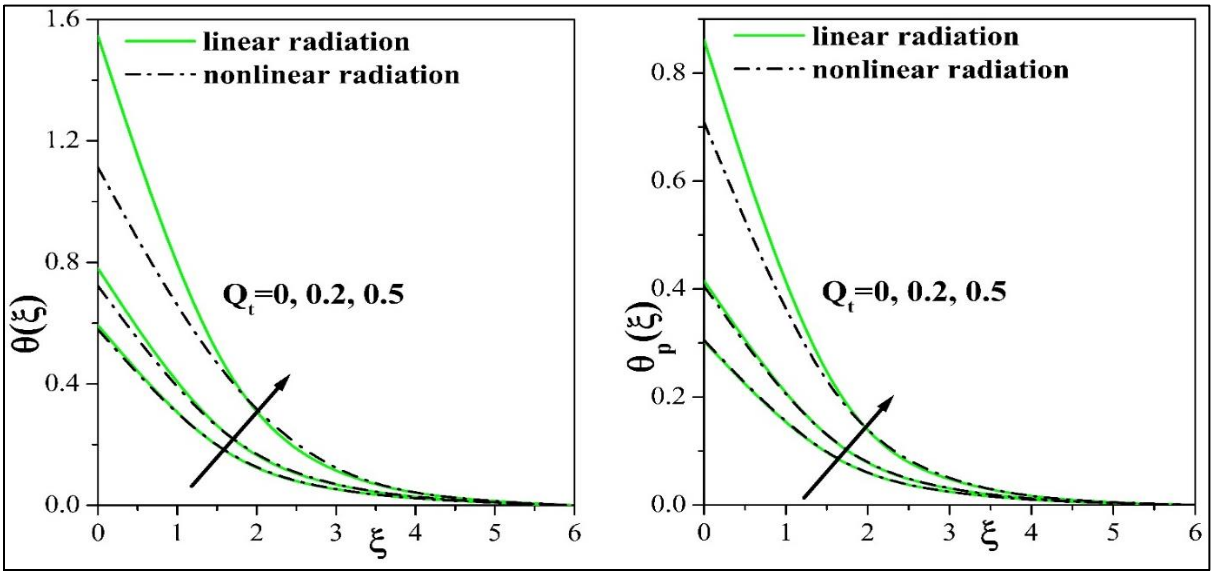

Fig 7 Influence of the Heat Source Parameter (Q_t) on the Temperature Distributions of the Fluid Phase $\theta(\xi)$ and Dust Phase $\theta_p(\xi)$.

ISSN No:-2456-2165 https://doi.org/10.38124/ijisrt/26aug1557

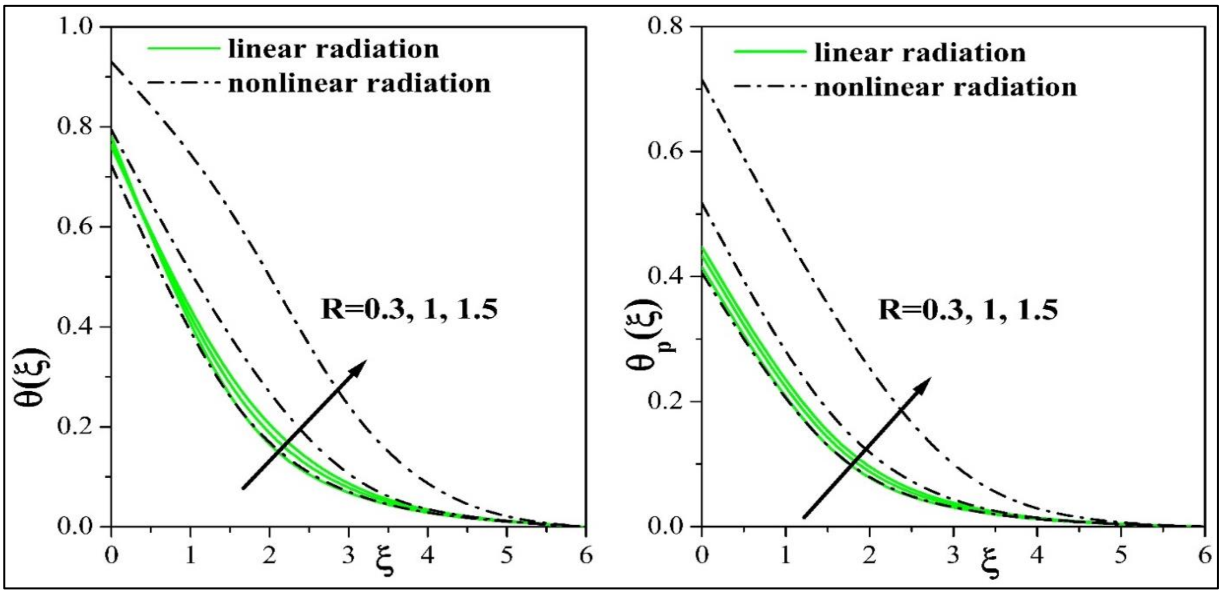

Fig 8 Influence of the Radiation Parameter (R) on the Temperature Distributions of the Fluid Phase $\theta(\xi)$ and Dust Phase $\theta_p(\xi)$.

➢ *Concluding Remarks*

The present study examined the effects of linear and nonlinear thermal radiation on MHD Casson dusty fluid flow over a convectively heated stretching sheet. Further considered the effects of exponential heat generation mechanisms and viscous dissipation. The governing PDE were transformed into ODE using suitable similarity transformations and solved numerically through the RKF shooting technique. The results revealed that increasing the Casson fluid parameter suppresses the fluid motion while enhancing the thermal field. It was further observed that larger values of the radiation parameter, Biot number, Eckert number, and heat generation parameters significantly increase the temperatures of both fluid and dust phases. Moreover, nonlinear radiation was found to produce considerably higher temperature distributions and heat transfer enhancement compared to linear radiation. The local Nusselt number increased with the radiation parameter, whereas stronger heat generation reduced the rate of heat transfer. Overall, the study demonstrates that nonlinear radiation plays a dominant role in enhancing the thermal characteristics of Casson dusty fluid flow, which is relevant to several engineering applications including thermal energy systems, solar collectors, cooling of electronic equipment, metallurgical processes, and particulate transport phenomena involving radiative heat transfer.

REFERENCES

[1]. Makinde, O. D. (2005). Free convection flow with thermal radiation and mass transfer past a moving vertical porous plate. *International communications in heat and mass transfer*, *32*(10), 1411-1419.

[2]. Mushtaq, A., Mustafa, M., Hayat, T., & Alsaedi, A. (2014). Effects of thermal radiation on the stagnation-point flow of upper-convected Maxwell fluid over a stretching sheet. *Journal of Aerospace Engineering*, *27*(4), 04014015.

[3]. Sreedevi, G., Rao, R. R., Rao, D. P., & Chamkha, A. J. (2016). Combined influence of radiation absorption and Hall current effects on MHD double-diffusive free convective flow past a stretching sheet. *Ain Shams Engineering Journal*, *7*(1), 383-397.

[4]. Gireesha, B. J., Kumar, P. S., Mahanthesh, B., Shehzad, S. A., & Abbasi, F. M. (2018). Nonlinear gravitational and radiation aspects in nanoliquid with exponential space dependent heat source and variable viscosity. *Microgravity Science and Technology*, *30*(3), 257-264.

[5]. Sampath Kumar, P. B., Pooja, C. P., & Sanjana, S. (2025). Three-Dimensional Slip Flow and Heat Transfer in Kerosene-Based Fe3O4 Ferrofluid Over a Nonlinear Stretching Sheet with Thermal Jump and Heat Generation Effects. *Journal of Nanofluids*, *14*(5), 688-696.

[6]. Jyoti, D. K., Nagaradhika, V., Sampath Kumar, P. B., & Mamatha, E. (2025). Three-Dimensional Heat Transfer in Radiative Oldroyd-B Nanofluid Flow with Irregular Heat Source and Activation Energy Effects. *International Journal of Applied and Computational Mathematics*, *11*(3), 110.

[7]. Pantokratoras, A., & Fang, T. (2013). Sakiadis flow with nonlinear Rosseland thermal radiation. *Physica Scripta*, *87*(1), 015703.

[8]. Cortell, R. (2014). Fluid flow and radiative nonlinear heat transfer over a stretching sheet. *Journal of King Saud University-Science*, *26*(2), 161-167.

[9]. Hayat, T., Imtiaz, M., Alsaedi, A., & Kutbi, M. A. (2015). MHD three-dimensional flow of nanofluid with velocity slip and nonlinear thermal radiation. *Journal of Magnetism and Magnetic Materials*, *396*, 31-37.

[10]. Mahanthesh, B., Kumar, P. S., Gireesha, B. J., Manjunatha, S., & Gorla, R. S. R. (2017). Nonlinear convective and radiated flow of tangent hyperbolic liquid due to stretched surface with convective condition. *Results in physics*, *7*, 2404-2410.

[11]. Ahmed, M. Z., Dhanalaxmi, V., & Thumma, T. (2025). Influence of nonlinear thermal radiation and exponential space dependent heat source on hybrid

ISSN No:-2456-2165 https://doi.org/10.38124/ijisrt/26aug1557

nanofluid stagnation point flow over a shrinking riga surface. *Multiscale and Multidisciplinary Modeling, Experiments and Design*, *8*(3), 175.

[12]. Abbas, M. S., Qamar, M., Khan, M., & Hussain, S. M. (2025). Chemically reactive flow of Williamson nanofluid with nonlinear thermal radiation over an exponentially stretching/shrinking surface. *Journal of Radiation Research and Applied Sciences*, *18*(3), 101630.

[13]. Gangadhar, K., Prameela, M., Chamkha, A. J., GR, B., & Kannan, T. (2026). Evaluation of homogeneous-heterogeneous chemical response on Maxwell-fluid flow through spiraling disks with nonlinear thermal radiation using numerical and regularized machine learning methods. *International Journal of Modelling and Simulation*, *46*(1), 100-122.

[14]. Ibtesam, M., Mengjie, S., & Ahmed, B. (2026). Significance of thermal jump in hybrid nanomaterial with nonlinear thermal radiation and porous space. *Partial Differential Equations in Applied Mathematics*, 101346.

[15]. Ireka, I. E. (2015). *Computational analysis of non-isothermal flow of non-Newtonian fluids*.

[16]. Fatahian, E., Kordani, N., & Fatahian, H. (2018). The application of computational fluid dynamics (CFD) method and several rheological models of blood flow: A review. *Gazi University Journal of Science, 31*(4), 1213–1227.

[17]. Fatahian, E., Kordani, N., & Fatahian, H. (2018). A review on rheology of non-Newtonian properties of blood. *IIUM Engineering Journal, 19*(1), 237–250.

[18]. Casson, N. (1959). Flow equation for pigment-oil suspensions of the printing ink-type. In C. C. Mill (Ed.), *Rheology of disperse systems* (pp. 84–104). Pergamon Press.

[19]. Mukhopadhyay, S., De, P. R., Bhattacharyya, K., & Layek, G. C. (2013). Casson fluid flow over an unsteady stretching surface. *Ain Shams Engineering Journal, 4*(4), 933–938.

[20]. Nandeppanavar, M. M., Vaishali, S., Kemparaju, M., & Raveendra, N. (2020). Theoretical analysis of thermal characteristics of Casson nanofluid flow past an exponential stretching sheet in Darcy porous media. *Case Studies in Thermal Engineering, 21*, 100717.

[21]. Awais, M., Raja, M. A. Z., Awan, S. E., Shoaib, M., & Ali, H. M. (2021). Heat and mass transfer phenomenon for the dynamics of Casson fluid through porous medium over shrinking wall subject to Lorentz force and heat source/sink. *Alexandria Engineering Journal, 60*(1), 1355–1363.

[22]. Walelign, T., Haile, E., Kebede, T., & Walelgn, A. (2020). Analytical study of heat and mass transfer in MHD flow of chemically reactive and thermally radiative Casson nanofluid over an inclined stretching cylinder. *Journal of Physics Communications, 4*(12), 125003.

[23]. Abo-Dahab, S., Abdelhafez, M., Mebarek-Oudina, F., & Bilal, S. (2021). MHD Casson nanofluid flow over nonlinearly heated porous medium in presence of extending surface effect with suction/injection. *Indian Journal of Physics, 96*(5), 1301–1315.

[24]. Reddy, B. N., & Maddileti, P. (2023). Casson nanofluid and Joule parameter effects on variable radiative flow of MHD stretching sheet. *Partial Differential Equations in Applied Mathematics, 7*, 100487.

[25]. Gubena, T., & Ibrahim, W. (2023). A 3D flow analysis of Casson nanofluid flow over a stretching surface with non-Fourier heat and non-Fick's mass flux. *International Journal of Thermofluids, 20*, 100488.

[26]. Ali, M. Y., Reza-E-Rabbi, S., Ahmmed, S. F., Nabi, M. N., Azad, A. K., & Muyeen, S. (2024). Hydromagnetic flow of Casson nanofluid across a stretched sheet in the presence of thermoelectric and radiation effects. *International Journal of Thermofluids, 21*, 100484.

[27]. Prakash, O. M., Makinde, O. D., Kumar, D., & Dwivedi, Y. K. (2015). Heat transfer to MHD oscillatory dusty fluid flow in a channel filled with a porous medium. *Sadhana*, *40*(4), 1273-1282.

[28]. Siddiqa, S., Begum, N., Hossain, M. A., Gorla, R. S. R., & Al-Rashed, A. A. (2018). Two-phase natural convection dusty nanofluid flow. *International Journal of Heat and Mass Transfer, 118*, 66-74.

[29]. Reddy, M. G., Rani, M. S., Kumar, K. G., Prasannakumar, B. C., & Lokesh, H. J. (2020). Hybrid dusty fluid flow through a Cattaneo–Christov heat flux model. *Physica A: Statistical Mechanics and its Applications*, *551*, 123975.

[30]. Kalpana, G., & Saleem, S. (2022). Heat transfer of magnetohydrodynamic stratified dusty fluid flow through an inclined irregular porous channel. *Nanomaterials*, *12*(19), 3309.

[31]. Das, S., Sarkar, S., Ali, A., & Jana, R. N. (2024). Exploration of magnetically influenced flow dynamics of a dusty fluid induced by the ramped movement of a thermally active plate. *Archive of Applied Mechanics*, *94*(2), 407-433.

[32]. Alahmadi, H., Rauf, A., Mushtaq, T., Tanveer, N., Omar, M., & Shehzad, S. A. (2024). Time-dependent double phase dusty fluid flow over an oscillatory rotating disk. *Heat Transfer*, *53*(3), 1336-1350.

[33]. Kumar, M. D., Raju, C. S. K., Sajjan, K., Dharmaiah, G., Shah, N. A., & Yook, S. J. (2025). Deep neural network-based prediction and computational fluid dynamics analysis of convective heat transfer in dusty fluid flow over heated surface. *Physics of Fluids, 37*(2).